PROCEEDINGS OF SCIENCE

Optimization of Spin Coherence at a Prototype Storage Ring for Electric Dipole Moment Measurements

Rahul Shankar[a,b,*], **Paolo Lenisa**[a,b] **and Andreas Lehrach**[c,d]

a Instituto Nazionale di Fisica Nucleare (INFN), Ferrara, Italy

b Università degli studi di Ferrara, Ferrara, Italy

c Forschungszentrum Jülich, 52425 Jülich, Germany

d RWTH Aachen University and JARA-FAME, 52056 Aachen, Germany

E-mail: shankar@fe.infn.it, lenisa@fe.infn.it

The JEDI experiment is dedicated to the search for the electric dipole moment (EDM) of charged particles using storage rings, which can be a very sensitive probe of physics beyond the Standard Model. In order to reach the highest possible sensitivity, a fundamental parameter to be optimized is the Spin Coherence Time (SCT), i.e., the time interval within which the particles of the stored beam maintain a net polarization greater than 1/e. To identify the working conditions that maximize SCT, accurate spin-dynamics simulations with the code BMAD have been performed on the lattice of a "prototype" storage ring which uses a combination of electric and magnetic fields for bending. This contribution will present an analysis of the mechanisms behind the decoherence, some techniques to maximize SCT through the optimization of second-order focusing parameters, and the exclusive beam and spin dynamics effects of the electric component of bending fields.

19th Workshop on Polarized Sources, Targets and Polarimetry (PSTP2022)
26-30 September, 2022
Mainz, Germany

*Speaker

PoS(PSTP2022)024

1 Introduction

Of all the observable matter antimatter asymmetry in the universe only a small fraction is accounted for by the currently accepted Standard Model (SM). Assuming the CPT theorem to hold true, it appears that this asymmetry can only be explained by additional CP violating processes than those accounted for in the SM [1]. A noticeable manifestation of CP violation is the presence of an Electric Dipole Moment in a proton, whose magnitude can indicate the existence of additional CP violation Beyond the Standard Model (BSM). While the SM predicts an EDM $\leq 10^{-31}\, e \cdot cm$, possible contributions from BSM theories could place it orders of magnitude higher. The current upper limit on the proton EDM is $7.9 \times 10^{-25}\, e \cdot cm$ [2].

The JEDI collaboration is currently working on performing this measurement using storage rings. EDM can be measured using a storage ring through precise observation of the interaction of particle spin with electric and magnetic fields. Since the EDM will point in the same direction as the spin, the presence of EDM will result in a torque on the particle in response to an electric field. The visible effect of this torque can be magnified using specially configured external electric fields. To achieve a precision higher than the current lower limit on the proton EDM, the construction of a dedicated storage ring would be needed [3] [4]. But before building such a ring, its feasibility must be demonstrated. So, to this end the JEDI collaboration will approach this problem in three stages [3]. The first stage involves experiments at the Cooler Synchrotron (COSY) in FZ, Jülich, with only magnetic bending fields. The second stage involves experiments in a prototype storage ring which uses a combination of electric and magnetic bending fields, featuring the possibilities of simultaneous counter-rotating beams and frozen spin.

Once the prototype has established the proof-of-principle, the final stage can be initiated, which would involve the measurement of the proton EDM at a purely electric storage ring, which would have the targeted precision to do so.

2 The Prototype EDM Storage Ring

In a storage ring that confines particles with a velocity $\vec{v}$ using an electric field $\vec{E}$ and a magnetic field $\vec{B}$ such that the three vectors are mutually perpendicular, the spins of the particles would undergo precession with respect to their velocity vectors due to the presence of a magnetic dipole moment (MDM), and an electric dipole moment (EDM). The frequency of this precession for a particle of mass m and charge q is given by the Thomas BMT equation [5]:

$$\begin{aligned}\frac{d\vec{\boldsymbol{s}}}{dt} &= -\frac{q}{m}\left[\left\{\left[\vec{\Omega}_{MDM}\right]_{rel}\right\} + \left\{\vec{\Omega}_{EDM}\right\}\right] \times \vec{\boldsymbol{s}} \\ &= -\frac{q}{m}\left[\left\{G\vec{B} + \left(G - \frac{1}{\gamma^2 - 1}\right)\vec{v} \times \vec{E}\right\} + \left\{\frac{\eta}{2}\left(\vec{E} + \vec{v} \times \vec{B}\right)\right\}\right] \times \vec{\boldsymbol{s}}\end{aligned} \quad (1)$$

The values of $\vec{E}$, $\vec{B}$ and the Lorentz factor γ can be set to make the relative precession due to the MDM ($\left[\vec{\Omega}_{MDM}\right]_{rel}$) vanish altogether. This is called "frozen spin" since in this configuration, the spin vector is aligned with the particle momentum at all times. Therefore, any torque on the particle's spin is now solely due to the EDM, and will point radially, causing a gradual build-up of vertical polarization among particles in the ring. The rate of this build-up will be proportional to the magnitude of the particle's EDM.

One such combination of fields is implemented for a ring with a bending radius of $12.25\ m$. The proposed design [6], shown in Figure 1 consists of four unit-cells, each with two bending dipoles, 4 quadrupoles and 4 sextupoles to provide sufficient flexibility in beam optics. The quadrupoles present on the ring are categorized into three families: QF (2 per unit cell, focussing),

QD (1 per unit cell, defocussing) and QSS (1 per unit cell, in the straight section). The sextupoles are placed on the same locations as the quadrupoles and are categorized into similar families: SXF, SXD and SXSS. Each family of magnets have a common power supply for centralized control. During this study however, the QSS magnets were turned off. An RF-cavity is also placed at one of the straight sections for bunching (longitudinal focussing) of particles.

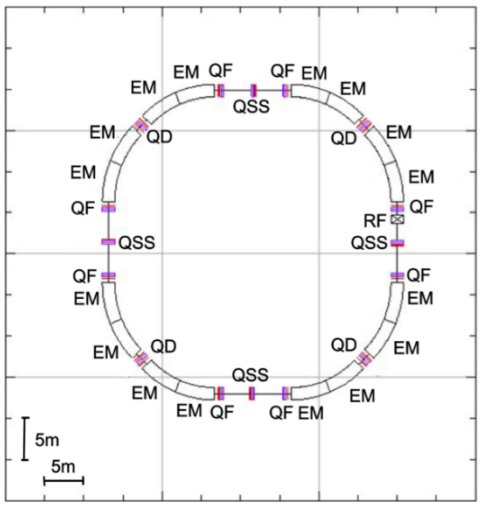

Figure 1: The software generated floor plan of the prototype EDM ring. Dipoles are labelled with 'EM', quadrupoles corresponding to their family with 'QF', 'QD' or 'QSS' and the cavity with 'RF'.

2.1 Spin Coherence time and Spin-Tune Error

Assuming a bunch of n particles are maintained in the storage ring, let $\hat{s}_i(t)$ be the unit vector in the direction of the i^{th} particle's spin vector. The polarisation vector $\vec{P}(t)$ is [6]:

$$\vec{P}(t) = \frac{1}{n}\sum_{i=1}^{n} \hat{s}_i(t) \qquad (2)$$

In a ring functioning in frozen-spin mode, if initially all particles distributed in phase space have their spins are aligned with their momenta ($|\vec{P}(0)| = 1$), the time τ taken for $|\vec{P}(\tau)| = \frac{1}{e}$ is defined as Spin Coherence Time (SCT). This quantity is ideal for evaluation of a storage ring for EDM measurements since very gradual polarization buildups would be noticeable only if the bunch remains spin-coherent. Therefore, longer SCT in a storage ring indicates a higher accuracy in potential EDM measurement. The spin tune spread $\Delta\theta_x$ measures the change in the direction of the polarisation vector from the reference particle in the plane of precession (here, assumed to be the ring plane):

$$\Delta\nu_s(t) = \frac{d}{dt}\left(\Delta\theta_x(t)\right) \approx \frac{d}{dt}\left(tan^{-1}\left(\frac{P_x(t)}{[\![s_z(t)]\!]}\right)\right) \qquad (3)$$

Here, P_x is the radial component of the polarization vector, and the hollow square brackets $[\![\ \ ]\!]$ indicate properties of the reference particle. Also interesting is the spin tune error $\Delta\nu_x(t)$, which is the rate of change of spin tune spread.

2.2 The Parameter Space

For the optimization of the Spin coherence time, the accessible parameter space consists of the field strengths k_F, k_D, of the two quadrupoles and $\chi_F, \chi_D, \chi_{SS}$ of the three sextupoles, labelled according to their corresponding families. However, the evaluation of the lattice in this study was carried out from the perspective of the optical parameters of the beam: namely the betatron tunes in each transverse direction Q_x, Q_y, the chromaticities ξ_x, ξ_y, and the momentum compaction factors of the first and second order α_0, α_1. While these are determined by the field strengths, the parameter space of the optics, at least in the first order represents the exhaustive set of configurations which result in real solutions to the Hill's Differential Equation (HDE) under the Courant-Snyder parameterization [8]. In other words, only dynamically "stable" beam configurations are included in the parameter space, represented in Figure 2. Scans in the second order, for a fixed first-order setting, reveal a bijective and linearly varying mapping between the space of sextupole field settings ($\chi_F, \chi_D, \chi_{SS}$) and second-order optical parameters (ξ_x, ξ_y, α_1).

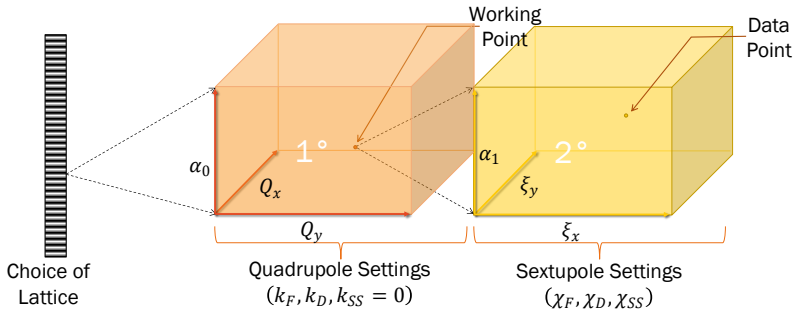

Figure 2: The organization of the parameter space explored in this study. The space formed by the betatron tunes Q_x, Q_y and the first-order momentum compaction factor α_0 is the first-order (1°) space, and the one formed by the chromaticities ξ_x, ξ_y and the second-order momentum compaction factor α_1 is the second-order (2°) space. A point in the first-order space is termed a working point, and one in the second-order space is termed a data point.

3 Results

Figure 3 demonstrates an instance of the time-development of the polarization as the particle bunch travels around the ring.

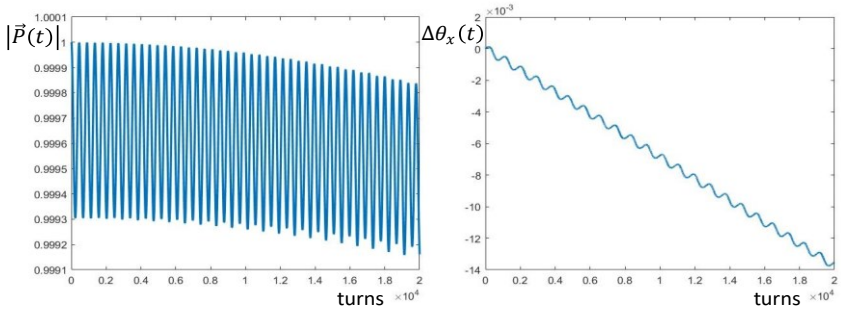

Figure 3: (left) A plot showing the decoherence of 1000 particles as a function of number of turns. (right) A plot showing the spin tune spread of the polarisation vector measured simultaneously.

From a detailed implementation of the Thomas-BMT equation on the prototype ring, it can be deduced that the change in the spin tune of an off-momentum particle stored in the ring would take the form (keeping terms up to the second order):

$$\Delta\nu_s = A\delta + B\delta^2 \qquad (4)$$

, where $\delta = {}^{\Delta p}/_{p}$ is the momentum offset of the particle, and A and B are constants which depend on the Lorentz factor γ, and the G-factor of the proton. Further, from the analyses in [9] and [10], the change in path length of the particle due to the contributions of both transverse and longitudinal motions is given by:

$$\frac{\Delta L}{L} = -\frac{\pi}{L}\left(\epsilon_x\xi_x + \epsilon_y\xi_y\right) + \alpha_0\delta + \alpha_1\delta^2 = \alpha_1\delta^2 - \frac{\pi}{L}\epsilon_x\xi_x - \frac{\pi}{L}\epsilon_y\xi_y \qquad (5)$$

…where the first-order longitudinal path-lengthening term is cancelled out in the long run by synchrotron oscillations. In general, path-lengthening effects manifest as an apparent speeding up of all particles with a non-zero emittance, which changes the effective Lorentz factor and thus the spin tune. This mechanism complements that of the momentum offset δ and can be observed in Figure 3 (right) showing the time development of the spin tune spread, where the local oscillations are due to the path-lengthening effect and the overall linear trend is due to the effective spin tune. Simulations at the origin ($\xi_x = 0$, $\xi_y = 0$, $\alpha_1 = 0$) show a downward trend without

local oscillations due to the effect of the δ^2 term in eq. (4). Measurements of the error in the spin tune measured at different points in the vector-space $\vec{\xi} = (\xi_x, \xi_y, \alpha_1)$ have shown that $\Delta\nu_s$ can be modelled as a scalar potential with a constant gradient, and that the set of all points with $\Delta\nu_s = 0$ forms a plane in this space. The plane thus represents the second order optical configurations where the path-lengthening effect cancels out the original spin tune error.

The Spin Coherence Time (τ) was estimated by fitting the data in Figure 3 (left) with the decoherence model derived in [11]:

$$|\vec{P}(t)| = |\vec{P}(0)|\left(\left[1 - \sqrt{\pi}\gamma_s(t)e^{-\gamma_s{}^2(t)}\,\mathrm{erfi}(\gamma_s(t))\right]^2 + \pi\gamma_s{}^2(t)e^{-2\gamma_s{}^2(t)}\right)^{\frac{1}{2}} \quad (6)$$

Here, n is the turn number and $\gamma_s(t) = \sqrt{2}\pi\sigma t$ is termed the "damping parameter" where σ can be obtained from the fit. From this model, τ is obtained by solving $|\vec{P}(\tau)| = {}^1/_e$.

It was observed that the variation of ${}^1/_{\tau^2}$ across the space follows the distribution of a three-dimensional paraboloid, specifically a family of ellipsoids,

$$\frac{1}{\tau^2} = \frac{1}{\tau_0{}^2} + L(\xi_x - \xi_x^o)^2 + M(\xi_y - \xi_y^o)^2 + N(\alpha_1 - \alpha_1^o)^2 + O(\xi_x - \xi_x^o)(\xi_y - \xi_y^o) + P(\xi_y - \xi_y^o)(\alpha_1 - \alpha_1^o) + Q(\alpha_1 - \alpha_1^o)(\xi_x - \xi_x^o) \quad (7)$$

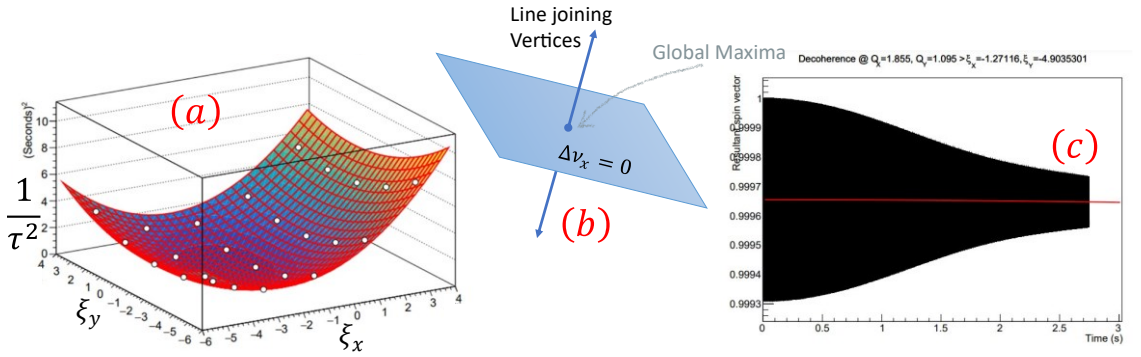

Figure 4: ***(a)*** *Inverse-square of spin-coherence time almost exactly varies as a 2D paraboloid (or a family of concentric ellipses). The vertex of the paraboloid represents the optimized field setting in the chosen 2D slice.* ***(b)*** *A diagram showing a possible method to estimate the SCT maxima as the intersection point between the $\Delta\nu_s = 0$ plane and the line joining the vertices of many 2D paraboloid fits.* ***(c)*** *A decoherence plot of the polarisation vector measured at the optimized point, showing almost no decoherence.*

…where L, M, N, O, P, Q are constants representing the geometric properties of the paraboloid, and ξ_x^o, ξ_y^o, α_1^o are the coordinates of the optimized point where the spin coherence time reaches its maximum value (τ_0) in a given quadrupole setting. This was also confirmed using 2D paraboloid fits at different slices of the space as shown in Figure 4 (a). It was expected that the maximum spin coherence time would occur in a setting where the effective spin tune is zero, given that this is a frozen-spin lattice. The simulation results demonstrate that this is always true and can reliably be used to narrow down the search during optimization as shown in Figure 4 (b).

Results of the optimization also show that the optimized settings always lie at negative chromaticities (like the example in Figure 4 (c)), which is contrary to the results at COSY [12], suggesting this may be an exclusive effect of the electric bending field.

Finally, optimization using these principles was performed at several quadrupole settings which exhibit optical properties within the recommended range in terms of beam lifetime [12] for this lattice, and spin coherence times of above $1000\,s$, which represents the target EDM sensitivity for the final lattice [3], was obtained at more than 10 points.

4 Conclusions

This paper presents the results of proton simulations at a storage ring in frozen-spin mode achieved using a combination of electric and magnetic bending fields. The results have demonstrated the optimisation of spin coherence times of above 1000 seconds at several working points in the prototype lattice. Also established is a robust method of optimisation which has demonstrated universality of working point, with successful optimisations at more than 90% of working points examined.

On the other hand, the study also highlights the limitations of this lattice in terms of optical flexibility, due to the placement of different sextupoles within the same straight section. Further studies shall explore new lattice configurations which could avoid these kinds of limitations.

5 References

[1] A. Sakharov, «Violation of CP invariance, C asymmetry, and baryon asymmetry of the universe,» *JETP Letters,* vol. 5, pp. 24-27, 1967.

[2] V. F. Dmitriev and R. A. Sen'kov, «Schiff Moment of the Mercury Nucleus and the Proton Dipole Moment,» *Physical Review Letters,* vol. 91, p. 212303, 2003.

[3] CPEDM Collaboration, «Storage ring to search for electric dipole moments for charged particles: Feasibility study,» CERN Yellow Reports: Monographs, Geneva, 2021.

[4] P. Lenisa, «Search for Electric Dipole Moments of Charged Particles with Polarized Beams in Storage Rings,» in *The 18th International Workshop on Polarized Sources, Targets, and Polarimetry*, Knoxville, 2019.

[5] V. Bargmann, L. Michel e V.L. Telegdi, «Precession of the polarization of particles moving in a homogeneous electromagnetic field,» *Physical Review Letters,* vol. 2, n. 10, p. 435, 1959.

[6] A. Lehrach, S. Martin e R. Talman, «Design of a Prototype EDM Storage Ring,» in *23rd International Spin Physics Symposium*, Ferrara, 2018.

[7] R. Shankar, M. Vitz e P. Lenisa, «Optimization of Spin Coherence Time at a Prototype Storage Ring for Electric Dipole Moment Measurements,» in *24th International Spin Symposium (SPIN2021)*, Matsue, 2022.

[8] S. Y. Lee, Accelerator Physics (Fourth Edition), Singapore: World Scientific, 2019.

[9] Marcel Stephan Rosenthal, «Experimental Benchmarking of Spin Tracking Algorithms for Electric Dipole Moment Searches at the Cooler Synchrotron COSY,» PhD Thesis, RWTH Aachen University, Aachen, 2016.

[10] Yoshihiko Shoji, «Dependence of average path length betatron motion in a storage ring,» *Physical Review Special Topics - Accelerators and Beams,* vol. 8, p. 094001, 2005.

[11] Dennis Eversmann, «High Precision Spin Tune Determination at the Cooler Synchrotron in Jülich,» PhD Thesis, RWTH Aachen University, Aachen, 2018.

[12] G. Guidoboni, E. J. Stephenson, A. Wrońska e et. al., «Connection between zero chromaticity and long in-plane polarization lifetime in a magnetic storage ring,» *Physical review accelerators and beams,* vol. 21, p. 024201, 2018.

[13] Saad Siddique, Andreas Lehrach e Jörg Pretz, «Simulations of Beam Dynamics and Beam Lifetime for a Prototype Electric Dipole Moment Ring,» in *24th International Spin Symposium (SPIN2021)*, Matsue, 2022.